Inter-Research Science Publisher

Marine Ecology Progress Series
Volume 754:77–92

Published February 13, 2025
https://doi.org/10.3354/meps14778

Larval connectivity for European green crab management in the Salish Sea and surrounding waters

Lilian Engel[1,*], Lakshitha Premathilake[1], Nicolas Barrier[2], Tarang Khangaonkar[1], Lysel Garavelli[1]

[1]Pacific Northwest National Laboratory, Coastal Sciences Division, 1100 Dexter Ave N, Seattle, WA 98109, USA
[2]MARBEC, University of Montpellier, CNRS, Ifremer, IRD, Sète 34203, France

ABSTRACT: The presence of invasive species is a growing concern in coastal marine ecosystems because of their adverse effects on biodiversity. The European green crab *Carcinus maenas* (EGC) is a small crab inhabiting inshore areas. Although it is native to the Northeast Atlantic Ocean and Baltic Sea, its distribution has expanded to North America, where it is an invasive species. Its main food sources are small invertebrate species that support valuable fisheries in the USA. The first presence of EGC in northern Washington was observed around 20 yr ago, along the Pacific Coast of the USA. Recently, EGC has been detected throughout the Salish Sea (Washington, USA, and British Columbia, Canada) wherein spread dynamics are unknown. The overall distribution of EGC is mainly driven by larval dispersal and, in the Salish Sea and surrounding waters, the assessment of EGC population dynamics is essential to understand its migration patterns and prevent its future expansion. To investigate the dispersal patterns of EGC larvae, a larval dispersal model was developed which couples a regional model of hydrodynamic circulation with an individual-based model of ichthyoplankton dynamics. Simulations were performed over 9 yr (2013–2022) to analyze average larval transport trends in the Salish Sea and surrounding waters, interannual variability of EGC larval connectivity, and the influence of larval behavior on connectivity patterns. Lastly, areas were identified to inform invasive species management moving forward. The prediction of likely sources and settlement locations of EGC larvae from the model will help improve the management of the population in the Salish Sea and surrounding waters.

KEY WORDS: Larval connectivity · Invasive species · Physical–biological interactions · Biophysical modeling

1. INTRODUCTION

Invasive species cost the global economy US $423 billion each year and play a key role in global plant and animal extinctions (Roy et al. 2023). Early detection and response are critical to prevent the establishment of invasive species, particularly in the marine environment. Since many successful marine invasive species, such as zebra mussels *Dreissena polymorpha*, European green crab (EGC) *Carcinus maenas*, and blue crab *Callinectes sapidus* have low mobility at the adult stage, the mechanisms of non-human facilitated invasion often occur during the early life stages. Thus, environmentally mediated invasion is often dependent on the oceanography of the region of interest because of the pelagic larval stage of many marine invasive species. Larval connectivity refers to the degree of interconnection among populations of a species through the exchange of larvae (Pineda et al. 2007, Lett et al. 2015). Connectivity is frequently applied in fisheries management because it effectively identifies the key geographic areas crucial for the sustainability of fisheries (Garavelli et al. 2016, Criales et al. 2019). Conversely, larval connectivity can help with the management of marine invasive species by identifying potential invasion pathways

*Corresponding author: lily.engel@pnnl.gov

Publisher: Inter-Research · www.int-res.com

and bottlenecks during this pelagic stage (Marchessaux et al. 2023).

The EGC is a small crab inhabiting inshore areas and is one of the most infamous marine invasive species, costing countries an estimated US $86.4 million since 1960 (Kouba et al. 2022). Although native to the Northeast Atlantic Ocean and Baltic Sea, its distribution has expanded to North and South America, Australia, and South Africa (Grosholz et al. 2021). Its main sources of food are small invertebrate species, such as clams, that support a valuable fishery in the USA. Evidence of habitat damage from EGC has been identified, such as impacts on seagrass beds (Matheson et al. 2016), which can lead to a decrease in fish and invertebrate abundance.

On the west coast of the USA along the Pacific coastline, the first presence of EGC was observed in northern California in 1989, originating from accidental human transport of east coast populations (Darling et al. 2008). The range expansion of EGC has since been northward along the US west coast, in the states of Oregon and Washington as well as in British Columbia, Canada. One of the explanations for the rapid expansion of EGC along the west coast could be the dispersal patterns of their early life stage. While adult EGC are benthic and do not travel long distances, their early life stage is pelagic and mobile (Grason et al. 2017). The transport of pelagic larvae is influenced by both physical (current velocities and directions, temperature) and biological factors (behavior, survival) (Pineda et al. 2007). The overall distribution of EGC along the US west coast is likely mainly driven by the dispersal of larvae from their spawning habitats to existing or new nursery (settlement) habitats.

EGC adults live 3 to 6 yr, typically breeding after 2 yr, with a relatively equal ratio of males to females within populations (Berrill 1982, Gillespie et al. 2015). Studies describing the EGC life cycle show a large range of fecundity (eggs released per female), from 185 000 eggs per female (Young & Elliott 2020) to 370 000 eggs per female (Leignel et al. 2014). The spawning period of EGC has mainly been inferred from observations of larvae and captures of adults. On the west coast of Vancouver Island (British Columbia, Canada), the highest densities of early-stage larvae were observed from April to August (DiBacco & Therriault 2015). This result is consistent with Banas et al. (2009), who inferred 2 peak spawning periods from captures of gravid females and sex ratios (Willapa Bay, Washington) in April–May and July–August. After hatching, larval settlement occurs within 4 to 9 wk, depending on water temperature (deRivera et al. 2007). In laboratory experiments, the duration from hatching to settlement was found to be 32 and 62 d at 18 and 12°C, respectively (Dawirs 1985), and 59 d at 12.5°C (deRivera et al. 2007). Field results provide similar observations, with development lasting 56 d at 13.5°C (Queiroga 1996). Temperature also influences larval settlement and recruitment. Observational studies report year-class recruitment failure when the mean water temperature (from December to March) is below 10°C (Behrens Yamada & Kosro 2010, Behrens Yamada et al. 2015). Based on the maximum duration of 13 d for the late larval stage of EGC (Dawirs 1985), 95% of larvae are competent to settle in 8 to 10 d (Zeng & Naylor 1996). All stages of EGC larvae exhibit diel vertical migration (DVM) behavior (Queiroga et al. 2002).

On the northwest coast of the USA, EGC have recently been detected in the Salish Sea, an inland sea contained by the state of Washington, USA, and British Columbia, Canada (Fig. 1). The Salish Sea is a glacially carved fjordal estuarine system with many narrow, long, and relatively deep interconnected basins that support strong currents induced by tides 3–4 m in range. Pacific Ocean tides propagate into the system in the southeast direction from the north via Queen Charlotte Strait and eastward via the Strait of Juan de Fuca (Fig. 1). The Strait of Juan De Fuca is the primary conduit between the inner Salish Sea and the Pacific Ocean that delivers exchange flow to the system as high as $100–150 \times 10^5\ m^3\ s^{-1}$ (Sutherland et al. 2011, Soontiens et al. 2016, Khangaonkar et al. 2017, Olson et al. 2021, MacCready & Geyer 2024). While the estuarine circulation structure of outflow through the surface and inflow through deeper layers may dominate (≈94% of the time in the summer and ≈55% of the time during the winter), affected by strong poleward winds and Eckman transport from the coast into the Salish Sea, the flow regime of the Strait of Juan de Fuca may change periodically (Thomson et al. 2007, Giddings & MacCready 2017). These transient effects reverse the circulation, with inflow occurring (counter-current) along the US Pacific Ocean coastline near the surface and outflow through the deeper layers, resulting in laterally shifted outflow along the Canadian coastline. The bathymetric features of the San Juan Islands and the Admiralty Inlet sill separate the Salish Sea into Georgia Basin in Canada and Puget Sound in US waters (Fig. 1).

The rapid invasion of EGC within the Salish Sea and surrounding waters has led to increasing research efforts to better understand their distribution and mitigate their expansion. Current management efforts of EGC include rigorous and expensive trapping of adult crabs by state agencies, Tribal Nations, and

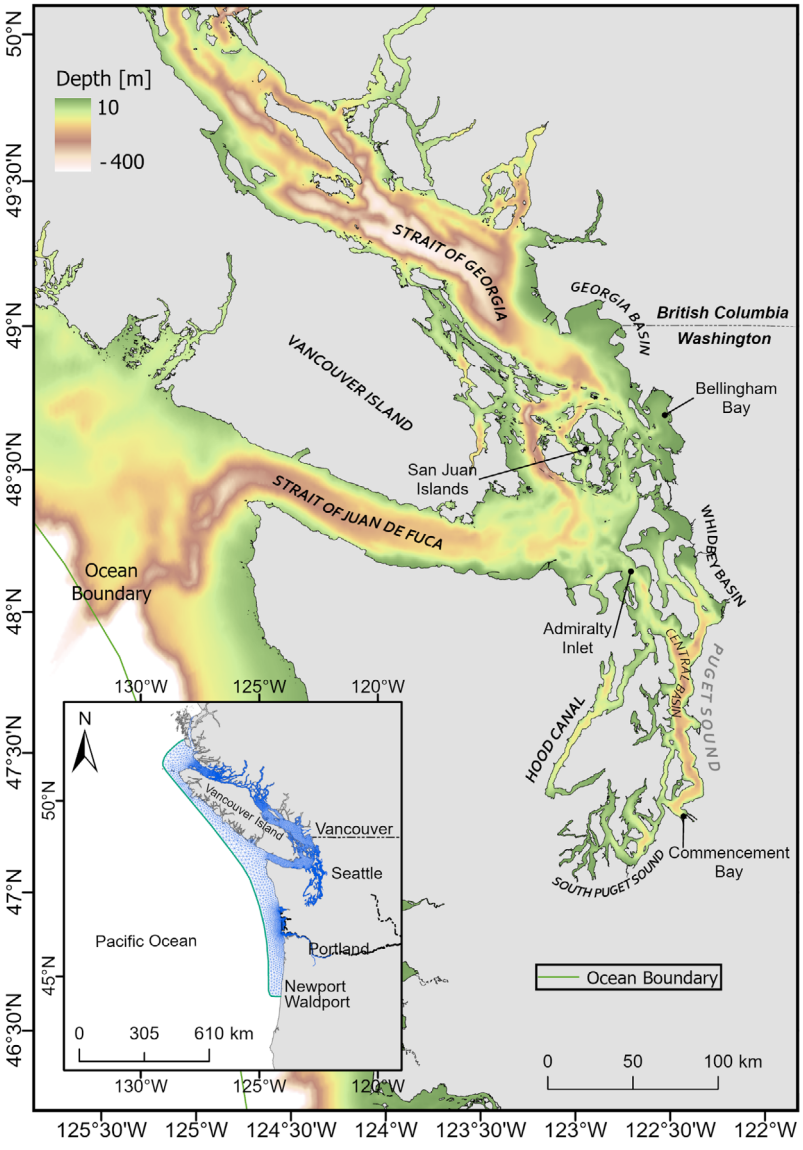

Fig. 1. Study domain including the mesh grid of the Salish Sea model (inset) (Khangaonkar et al. 2018) and zoomed in on the Puget Sound/Strait of Georgia. Image reproduced with permission from Premathilake & Khangaonkar (2022)

other organizations in the region, including volunteer and citizen science efforts (Grason et al. 2018, WDFW 2024). However, to aid the existing management of the EGC population in waters in and around the Salish Sea and prevent its expansion, there is a need to understand the migration mechanisms and patterns of the species. Larval dispersal modeling studies of EGC in the region highlighted mechanisms by which EGC could have entered the Salish Sea (Brasseale et al. 2019, Du et al. 2024). Specifically, they found that larvae could be carried into the Salish Sea during the late cold season when a regular flow reversal of the Strait of Juan de Fuca occurs (Behrens Yamada et al. 2017, Brasseale et al. 2019, Du et al. 2024). While these studies effectively assess the pathways for the initial EGC larval invasion into the Salish Sea (Brasseale et al. 2019) and transport dynamics within the Salish Sea (Du et al. 2024), further management of this invasive species would benefit from a study focusing on EGC larval connectivity patterns within the Salish Sea.

Using a biophysical larval dispersal model, we investigated EGC larval connectivity patterns within the Salish Sea and surrounding waters to aid the management efforts of this invasive species. We investigated larval trajectories and connectivity matrices over 9 yr (2013–2022) of simulation time to analyze larval transport patterns in the Salish Sea and surrounding waters, interannual variability in EGC larval connectivity, and the influence of larval behavior on connectivity patterns. Lastly, areas are identified from EGC larval connectivity patterns for the future management of this invasive species.

2. METHODS

2.1. Biophysical larval dispersal model

2.1.1. Hydrodynamic model

The Salish Sea model (SSM) used in this study covers the entire Salish Sea, including Puget Sound, the Strait of Georgia, the Strait of Juan De Fuca, the waters surrounding Vancouver Island, and the continental shelf, as shown in Fig. 1. It is a comprehensive model that uses the Finite Volume Community Ocean Model (FVCOM) framework to solve Reynolds-averaged Navier-Stokes equations for turbulent flows in coastal ocean environments (Chen et al. 2003). The hydrodynamic solutions are generated using a finite volume framework with an unstructured grid with lateral resolution that varies from a cell size of ≈250 m near river mouths to ≈800 m in Puget Sound, increasing to ≈3 km resolution in the straits and 12 km over the

continental shelf (see grid lines in Fig. 2b). The vertical configuration of the model uses 10 sigma-stretched layers distributed using a power law function with an exponent P-Sigma of 1.5, which provides more layer density near the surface. The SSM, including the hydrodynamic component of the model, has been calibrated over a multi-year simulation from 2013 to 2020 (Khangaonkar & Yun 2023). The model performance is compliant with the targets established by the local user community ($RMSE_T$ <1°C, $RMSE_S$ <1 psu, and RMSE for water surface elevation <10% relative to tidal range). Outputs are saved hourly.

2.1.2. Larval dispersal model

The Lagrangian model Ichthyop (Lett et al. 2008, Barrier et al. 2023) is commonly used to model transport processes and assess the effects of hydrodynamics on plankton dynamics (Garavelli et al. 2014, 2016, Marchessaux et al. 2023, Amorim et al. 2024). In this model, adult spawning locations and larval settlement locations are defined by longitude, latitude, and bathymetry. While accounting for the biological larval characteristics, the model tracks the larvae in 3 dimensions by their latitude, longitude, and depth. The SSM-generated hydrodynamics were externally (offline) coupled with Ichthyop to model the larval dispersal of EGC in the Salish Sea and surrounding waters. Although Ichthyop has native built-in support to direct external coupling with hydrodynamics from the Regional Ocean Modeling System (ROMS) (Lett et al. 2008), the current version does not possess the capability for coupling hydrodynamics from models based on an unstructured grid framework such as FVCOM. To overcome this challenge, a new computational framework was developed in Ichthyop to couple the SSM hydrodynamic solutions. Being a Lagrangian model, Ichthyop is flexible in utilizing the input information (hydrodynamics) distributed in any spatial scale or structure. Hence, a new spatial interpolation scheme was developed in Ichthyop for extracting the gridded data distributed on a triangular unstructured 2D mesh using linear shape functions defined separately for cell-centric vector fields and node-centric scalar fields. Ichthyop uses the 3-dimensional current field and water surface elevations from SSM to drive the transport of larvae. The larval dispersal model is run in 30 min timesteps and then saved every 10 h. In addition to hydrodynamic inputs, Ichthyop requires biological and ecological information on EGC in the Salish Sea for larval dispersal model setup and calibration/validation purposes. The relevant parameters used in this study are detailed below and summarized in Table 1.

Spawning and settlement locations of EGC were defined based on geographic features in the Salish

Table 1. Summary of the biological parameters included in the European green crab larval dispersal model

Parameter	Description	Definition	Reference
Spawning locations	Locations where larvae are released/spawned	See Fig. 2	Grason et al. (2018)
Settlement zone	Zones where larvae may settle	See Fig. 2	Grason et al. (2018)
Spawning depth	Depth where larvae are released/ spawned	0–30 m	Grason et al. (2018)
Spawning time	Day on which larvae are released from the spawning zones per release event	1 April, 1 May, 1 June, 1 July, 1 August	Banas et al. (2009), DiBacco & Therriault (2015)
Years studied	Years of model simulation	2013–2022	
Larval behavior	Diel vertical migration (DVM) of zoeae I–IV, only implemented in duplicate simulations run in 2017 and 2020 in this study	Passive in all simulations; when implemented in duplicate 2017 and 2020 simulations, DVM is 3 m sunset and 15 m sunrise	Queiroga et al. (2002), DiBacco & Therriault (2015)
Laval dispersal duration	Amount of time larvae are transported during each simulation	65 d	Dawirs (1985), deRivera et al. (2007)
Pre-competency period	Age limit before larvae can settle in a settlement zone	30 d	Dawirs (1985), Zeng & Naylor (1996)
Spawning event	Number of larvae released each spawning time	10 000 larvae per release event	Brasseale et al. (2019)

Sea and within 1 grid cell of the hydrodynamic model along the coastline because EGC are primarily distributed along the coast. For each spawning event, a total of 10 000 virtual EGC larvae were released from within the defined spawning zones (Fig. 2). In the individual-based model (Ichthyop) used in our study, the number of larvae to release per zone depends on the surface area in that zone and the total eligible release zone surface area. The number of larvae is then randomly released within that release zone (Lett et al. 2008, Barrier et al. 2023). The model of Brasseale et al. (2019) released 10 000 particles per simulation to save computation time and provide sufficient data for their purposes. In our model, simulations with 100 000 larvae resulted in qualitatively similar outputs to 10 000. Larvae were released within the top 0–30 m of the water column, as defined in the hydrodynamic outputs, because EGC are observed in shallow coastal waters (Grason et al. 2018). To reflect the higher density of EGC observed in the summer months (Banas et al. 2009, DiBacco & Therriault 2015), in the model, larvae were released at midnight on 1 April, 1 May, 1 June, 1 July, and 1 August of the study years 2013–2022. Thus, this study reports on the results of 50 release events (5 yr^{-1} for 10 yr). In the model of Brasseale et al. (2019), the larval dispersal duration of EGC was set between 30 and 75 d. In our model, the maximum larval dispersal duration is 65 d and the pre-competency period (time at which larvae can settle) is 30 d. Larvae that reach a settlement zone between 30 and 65 d after the spawning event are considered 'successfully settled'. The surface temperature of the Salish Sea is typically above 10°C for the months investigated in this study (Khangaonkar et al. 2018), and therefore mortality of larvae related to temperature was not considered (see Fig. S1 in the Supplement at www.int-res.com/articles/suppl/m754p077_supp.pdf). Larvae that reached the boundary of the hydrodynamic domain were recorded as dead and stopped moving.

Our study primarily focuses on passive transport of EGC larvae and thus does not include DVM for the years 2013–2022. However, to compare larval dispersal patterns of EGC with and without larval behavior, DVM was included in our model following the models of Brasseale et al. (2019) and Du et al. (2024) for a duplicate run of the years 2017 and 2020. In the models of Brasseale et al. (2019) and Du et al. (2024), the vertical positions of the larvae were set at 3 m at night (starting at sunset, 21:00 h) and 15 m during the day (starting at sunrise, 05:00 h), which was consistent with field observations in British Columbia (DiBacco & Therriault 2015).

2.2. Analysis of model outputs

Connectivity matrices were primarily used to interpret the model results. A connectivity matrix $\boldsymbol{C}_{ij}$ was calculated as the number of particles released from area j that are transported to area i. To account for the random release of larvae, the percentage of larval transport success between 2 zones was calculated as $\boldsymbol{C}_{ij}$ normalized to the total larvae released per zone, $\frac{C_{ij}}{n_i} \times 100$ where n_i is the number of larvae released in zone i. The total percentage of successfully settled larvae in a given settlement zone was calculated as the row sum of the matrix normalized to the number of larvae released, or $\sum_j \frac{C_{ij}}{N} \times 100$ where N is the total larvae released per event, i.e. 10 000. The total percentage of successfully settled larvae from a given release zone was calculated as the column sum of the matrix normalized to the number of larvae released, or $\sum_i \frac{C_{ij}}{N} \times 100$

Lastly, annual transport success percentage was calculated by summing all values in each annual connectivity matrix and then normalizing to the total larvae released, $\sum_i \sum_j \frac{C_{i,j}}{N} \times 100$

Further analysis of the connectivity results using the method of Jacobi et al. (2012) was performed to identify potential management areas in this region. This method divides the domain into smaller areas by minimizing a larval exchange objective function of the zones in the connectivity matrix and has been used in other studies (Garavelli et al. 2016, Muller et al. 2024). Identifying highly independent areas is relevant for invasive species management.

3. RESULTS

3.1. Larval trajectories

Larval trajectories over time are presented here via a density plot at time 0 d (release) and time 65 d of the simulation for all study years (Fig. 3) and trajectories of 1 release event in the entire domain and specific zones (Fig. 4). Fig. 3 shows that there is a higher density of larvae inside the Salish Sea than outside on Day 0 (Fig. 3a), but a higher density of successfully settled larvae outside of the Salish Sea than inside on Day 65 of larval dispersal duration (Fig. 3b). Due to the random release of larvae in the

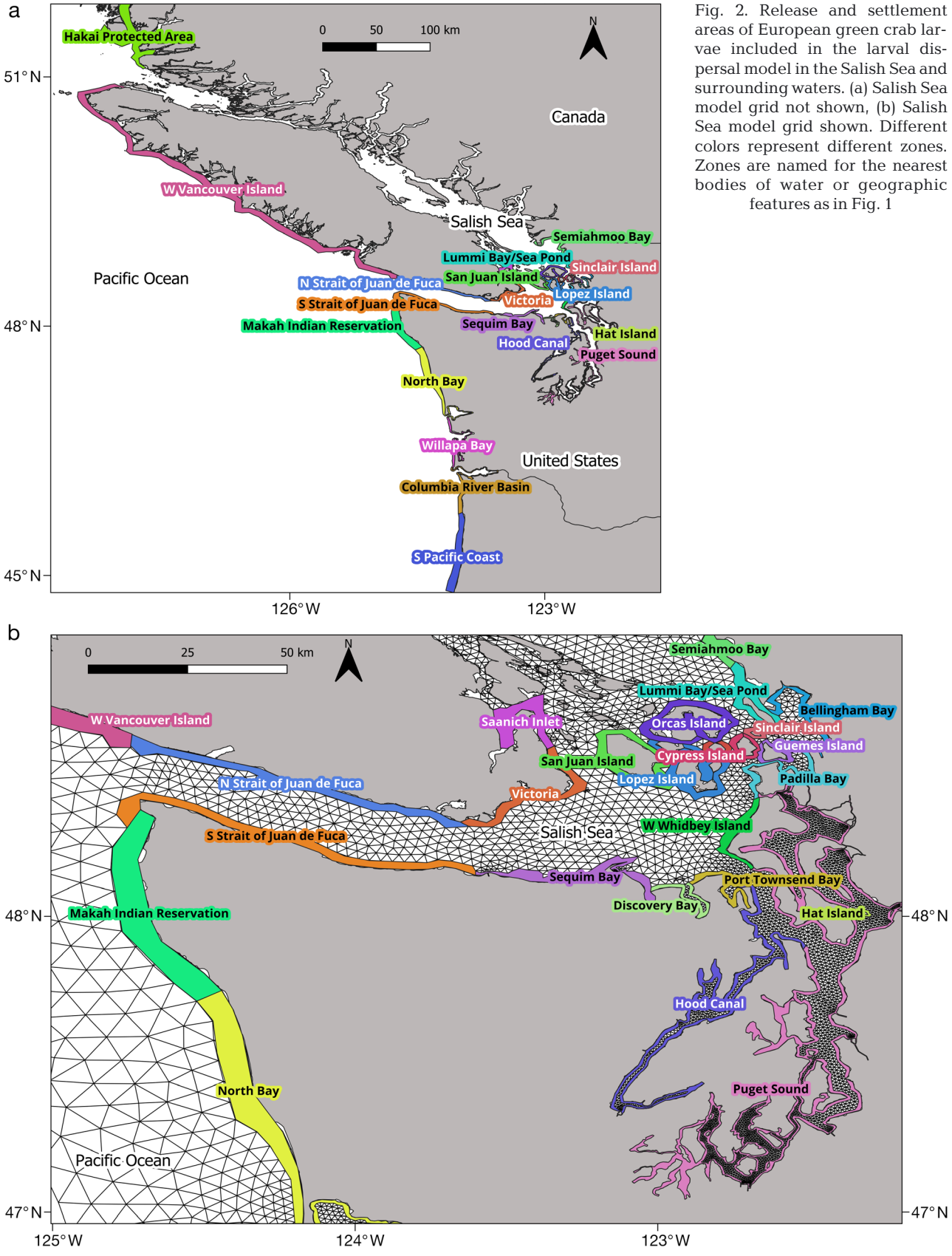

Fig. 2. Release and settlement areas of European green crab larvae included in the larval dispersal model in the Salish Sea and surrounding waters. (a) Salish Sea model grid not shown, (b) Salish Sea model grid shown. Different colors represent different zones. Zones are named for the nearest bodies of water or geographic features as in Fig. 1

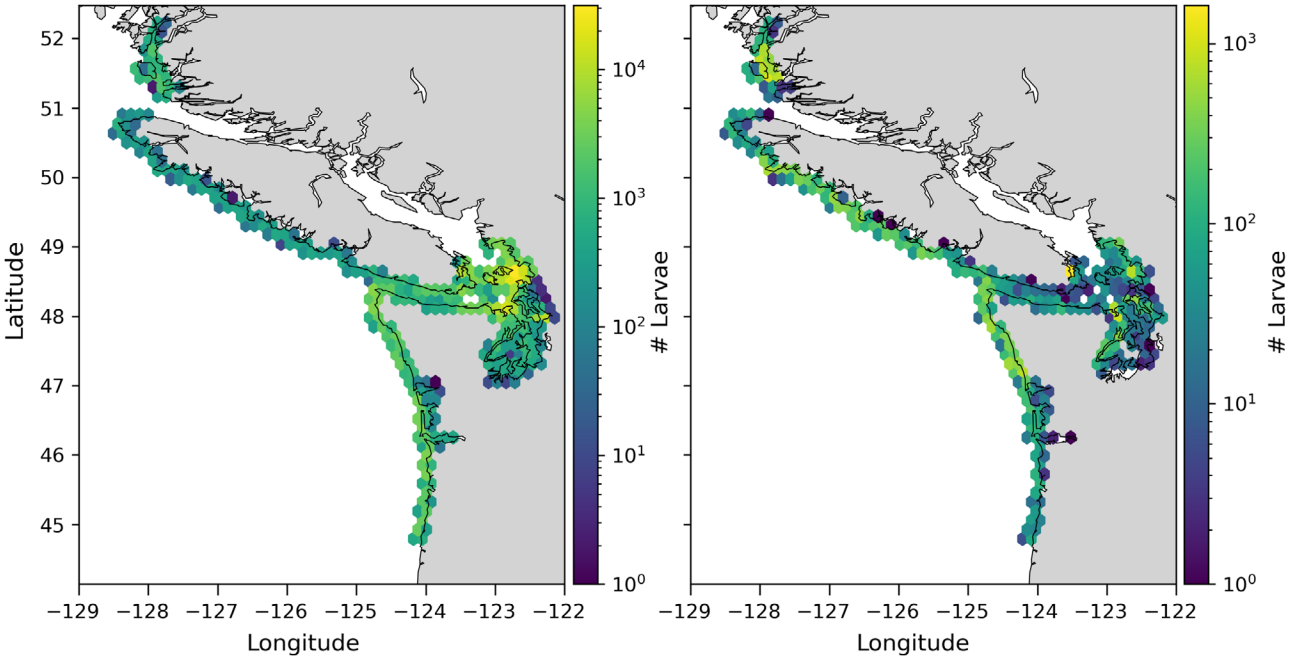

Fig. 3. Densities of European green crab larvae after (a) 0 and (b) 65 d of larval dispersal duration. Panel (a) shows the density of all larvae released, and (b) shows the density of successfully settled larvae only (those reaching a settlement zone between 30 and 65 d after release). These plots include data from all simulations from 2013–2022

model, the San Juan Islands region (48.5° N, 123° W) and the Washington coast (45–48° N, 124° W) released relatively more larvae than other regions (Fig. 3a). Larvae which successfully settle (Fig. 3b) are more concentrated on the northern Washington coast, West Vancouver Island (49° N, 127° W), and the Hakai Protected Area region (51.5° N, 128° W). Larval density changes at the end of 65 d of larval dispersal duration (Fig. 3b) indicate that larvae either travel from within the Salish Sea to the Pacific Ocean or do not successfully settle within the Salish Sea.

The trajectories of successfully settled larvae from the release event on 1 April 2020 (Fig. 4a) show a similar phenomenon: larvae within the Salish Sea move outside the Salish Sea over time. Larvae within constrained regions such as the Hakai zone (Fig. 4b), Hood Canal (Fig. 4c) zone, or various zones within the San Juan Islands region (Fig. 4d) become trapped and are unable to move outside of their respective zones with time. The Hakai zone is at the northern boundary of our model, so no larvae are moving west of the zone (between the island and the mainland). However, this should not influence model results because larvae that would move toward this direction would beach at the model boundary and stop moving, and would therefore not be considered successfully settled into the zone.

3.2. Larval connectivity

Larval connectivity patterns were analyzed to further understand the favorable spawning and settlement zones of EGC. The average connectivity matrix of the entire study period 2013–2022 shows high larval connectivity between the coastal zones (Makah, North Bay, Willapa Bay, Columbia River, and S Coast) (Fig. 5), evidenced by the clustering in the figure. High larval connectivity is also observed in the San Juan Islands region (Fig. 4d; San Juan Island, Lummi Bay, Semiahmoo Bay, Bellingham Bay, Orcas Island, Lopez Island). Western Vancouver Island receives the most larvae and is the only settlement zone with at least some larvae from all of the release zones. The North and South Strait of Juan de Fuca, Sequim, and Makah zones receive larvae from most release zones. For most of the zones, there is also strong local retention, when larvae settle in the same zone in which they are released (diagonal line of the connectivity matrix). The Hakai zone had the largest amount of local retention, which is also the largest transport success rate in the matrix. The fewest larvae settled in the Hat Island and Blakely Island zones during the study period. There is higher larval transport success in the bottom right quadrant of the connectivity matrix (larvae that leave the Salish Sea and enter the Pacific Ocean) than in the top left quadrant (larvae that enter the Salish Sea from the Pacific Ocean).

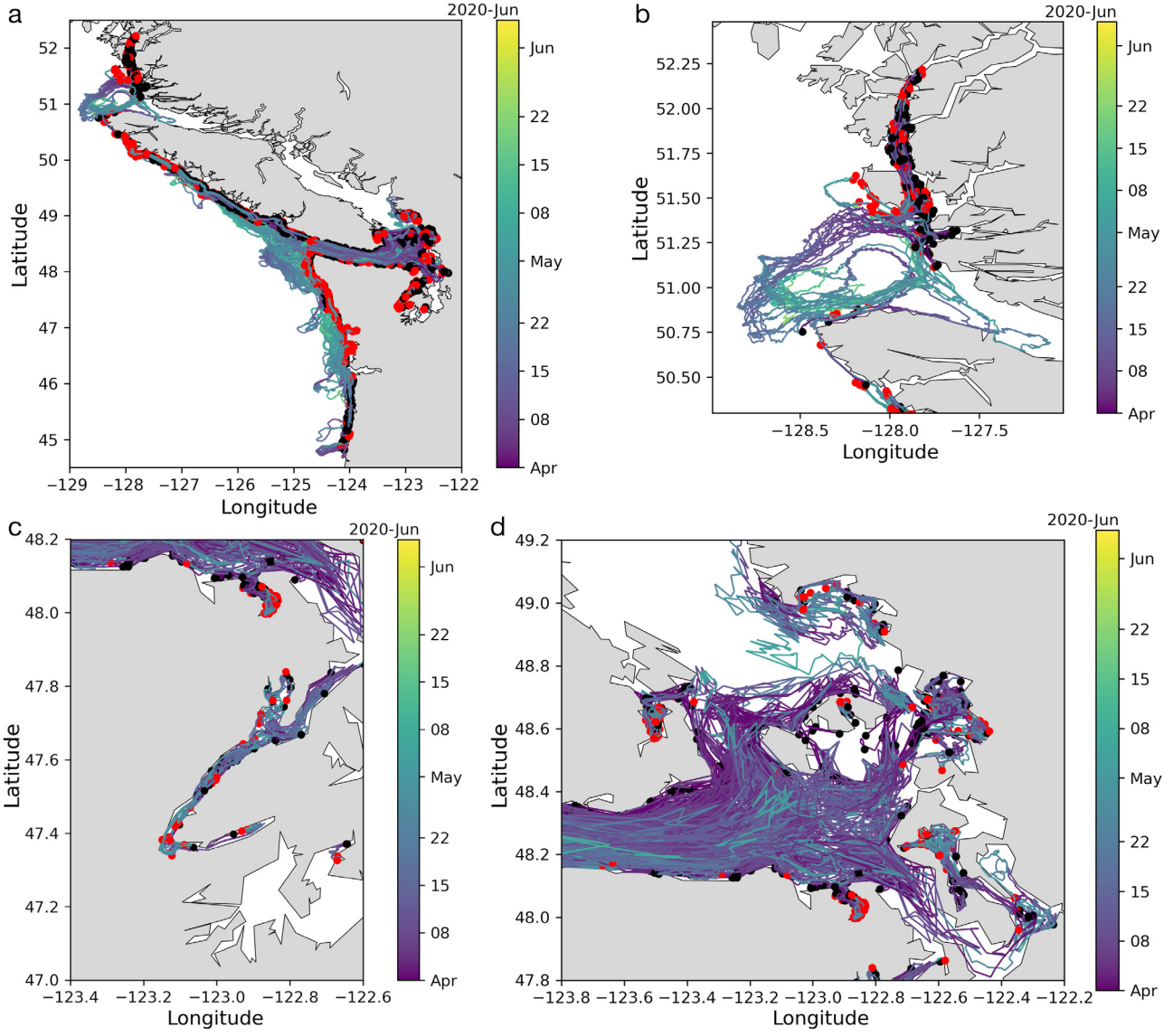

Fig. 4. Trajectories of successfully settled European green crab larvae released on 1 April 2020, for 65 d of simulation time in (a) the entire domain, and zoomed in on (b) the Hakai and (c) Hood Canal release/settlement zones or (d) the San Juan Islands region. Release and settlement zones of note in the San Juan Islands region include Saanich Inlet, San Juan Island, Orcas Island, Bellingham Bay, and Lummi Bay. Color goes from purple to yellow to represent simulation time. Black dots represent the release locations, red dots represent the settlement locations

3.3. Interannual variability

The sum of the connectivity matrices for each year (normalized to all larvae released) reveals interannual variability in our data set. Fig. 6a shows that larval settlement varies annually in W Vancouver Island by up to ±3.2%, North Bay by up to ±1.5%, and Makah Indian Reservation and Hakai by up to ±1%. The rest of the settlement zones varied by less than ±0.5%. Regardless of the year, W Vancouver Island and Hakai Protected Area always receive more larvae than the other zones. The larval transport success is low in Sinclair, Cypress, Blakely, and Lopez Islands across the years.

Fig. 6b shows that larvae released from each zone tend to settle somewhere, even though not every settlement zone receives larvae (Fig. 6a). This is particularly evident for the Cypress, Sinclair, Lopez, and Blakely Islands zones: larvae do not always settle in these zones (Fig. 6a), but larvae originating from these zones are successfully transported (Fig. 6b). For all other release zones, the inter-annual variability of larval transport success is low. For example, while Hakai Protected Area had reduced transport success

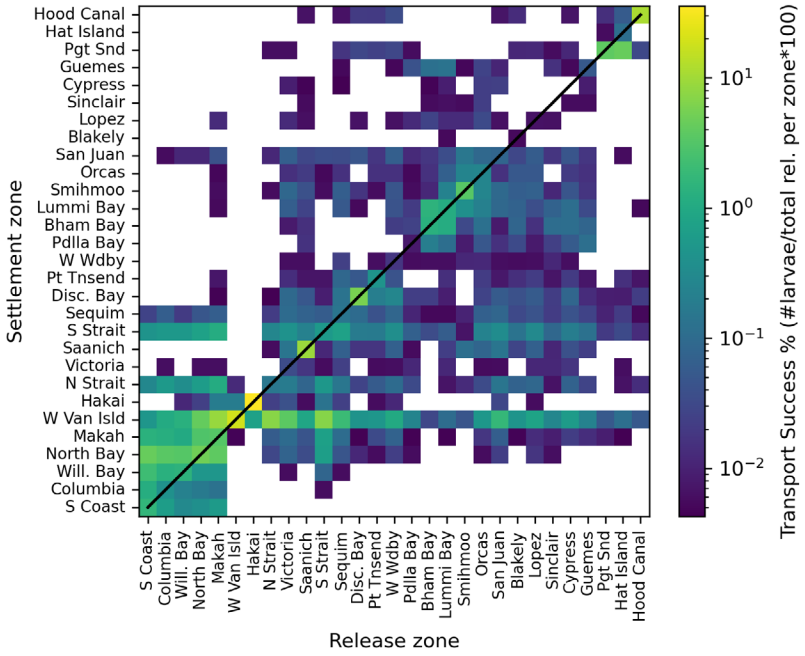

Fig. 5. Connectivity matrix for successfully settled European green crab larvae after 65 d of dispersal. Larvae were released on the first of April, May, June, July, and August for each year of 2013–2022 and then averaged by the number of release events (50). Values of the connectivity matrix ***Cij*** are calculated as the number of particles released from area *j* that are transported to area *i*. The transport success is calculated by normalizing ***Cij*** to the total larvae released per zone. Names shortened to fit on the matrix but correspond to zones in Fig. 2. Abbreviations of the release/settlement zones are defined in Table S1

in 2017 compared to other years and W Vancouver Island had reduced transport success in 2016 and 2017, other zones do not have much variation from year to year.

Fig. 6c shows the annual variability of the total transport success of EGC larvae across all zones. Total transport success is calculated by summing rows of either Fig. 6a or Fig. 6b or all values in Fig. 5. Transport success increased from 2013 to 2014 and 2016 to 2019, and decreased from 2015 to 2016 and 2019 to 2022. The maximum transport success occurred in 2019, with over 9% of larvae successfully settled (i.e. 91% of larvae did not settle), whereas the lowest transport success occurred in 2016, with 5% of larvae successfully settled (i.e. 95% of larvae did not settle).

3.4. Inclusion of larval behavior

The inclusion of DVM behavior in the larval dispersal model for 2020 slightly changes the connectivity patterns (Fig. 7). In general, there is more transport success without DVM, noted by the red boxes in the difference connectivity matrix (difference obtained as: passive larvae connectivity − DVM connectivity). Connectivity is higher between the S Coast and Columbia River with DVM. Larvae settle with slightly higher success without DVM on the coast, and larvae settle in the San Juan Region with comparable levels of success with and without DVM. Including DVM reduces the local retention of Hakai and West Vancouver Island. Total average transport success (sum of the entire matrix) in 2020 was 8.53% without DVM and 5.44% with DVM. A duplicate run in 2017 gave similar results (see Fig. S2). Total transport success in 2017 was 5.53% without DVM and 4.67% with DVM. The largest difference in connectivity is observed in the local retention in the Hakai zone.

3.5. Identification of highly connected areas

Using the larval connectivity results from the model, 8 highly connected areas of EGC were identified in the region (Fig. 8). One independent highly connected area is identified between the Canadian and US parts of the Strait of Juan de Fuca, West Vancouver Island (Canada), and the southern San Juan Islands (USA). The Pacific Coast is also highly connected. The largest connectivity is noted between the Makah zone and the Strait of Juan de Fuca (17%), highlighting that those areas are less independent than others which have larval exchange below 10% (Fig. 8). The highest local retention of the independent highly connected areas occurs in the Pacific Coast, Puget Sound, Hood Canal, and Hakai zones. Additionally, our results suggest 4 independently connected areas within the North Puget Sound. The areas identified in Fig. 8 have an average larval exchange with each other of 19%.

4. DISCUSSION

The results of this study provide important information for the management of the invasive EGC in the Salish Sea and surrounding waters. Overall patterns in our results indicate that larvae tend to move from the Salish Sea to the Pacific Ocean, there is interannual

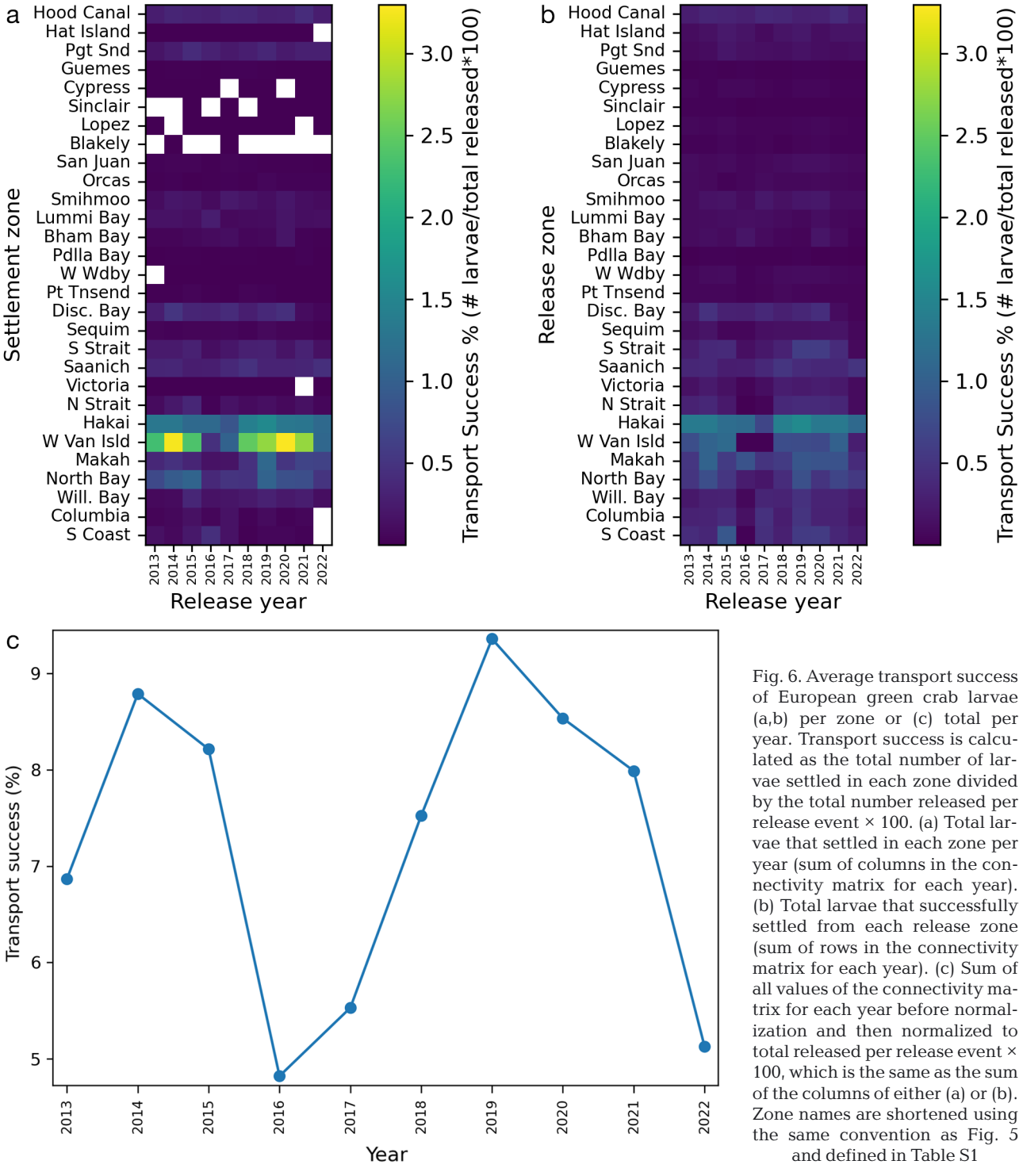

Fig. 6. Average transport success of European green crab larvae (a,b) per zone or (c) total per year. Transport success is calculated as the total number of larvae settled in each zone divided by the total number released per release event × 100. (a) Total larvae that settled in each zone per year (sum of columns in the connectivity matrix for each year). (b) Total larvae that successfully settled from each release zone (sum of rows in the connectivity matrix for each year). (c) Sum of all values of the connectivity matrix for each year before normalization and then normalized to total released per release event × 100, which is the same as the sum of the columns of either (a) or (b). Zone names are shortened using the same convention as Fig. 5 and defined in Table S1

variability between the transport success of larvae settlement, and including larval behavior in the model slightly decreases larval settlement. In the following section, we investigate these trends and discuss the new EGC management areas based on further analysis of our larval connectivity results.

Larval trajectories and connectivity indicate that larvae tend to disperse from the Salish Sea to the Pacific Ocean and rarely enter the Salish Sea from the Pacific Ocean. This pattern matches the overall flow of the Strait of Juan de Fuca: during the months of the study (i.e. April–October), fresh water primarily (90%

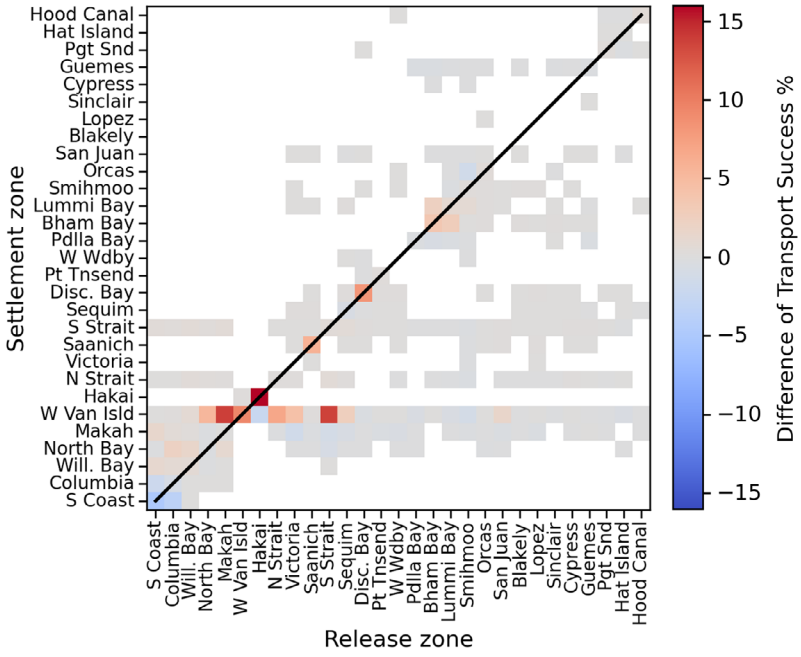

Fig. 7. Difference of 2020 average connectivity matrices without and with diel vertical migration (DVM). Positive values (red) indicate that there is a greater transport success without DVM while negative values (blue) mean that there is greater transport success with DVM. The larval transport success from one release zone to one settlement zone is calculated over the 5 spawning events on the first of April, May, June, July, and August 2020. When implemented, DVM is set to −15 m during the day and −3 m at night. Zone names are shortened using the same convention as Fig. 5 and defined in Table S1

of the time) flows out of the Salish Sea towards the Pacific Ocean on the surface, and saltwater flows in at depth (Thomson et al. 2007). In the winter months (November–March), there are occasional shifts in the flow direction of the Strait of Juan de Fuca (Thomson et al. 2007, Giddings & MacCready 2017). This circulation feature in the Strait of Juan De Fuca with short duration (a few days to weeks) reversals likely offers a mechanism for transporting EGC larvae into the Salish Sea (Brasseale et al. 2019, Du et al. 2024). In our model, only summer spawning months are included and most of the larvae remain near the surface; larvae follow the usual trajectory of the Strait, as is primarily observed in other modeling studies of the region (Brasseale et al. 2019, Du et al. 2024). However, despite strong salinity gradients and stratification, the presence of circulation cells and bathymetry-induced vertical mixing provides opportunities for surface water to be refluxed into bottom layers. Thus, if a larva was

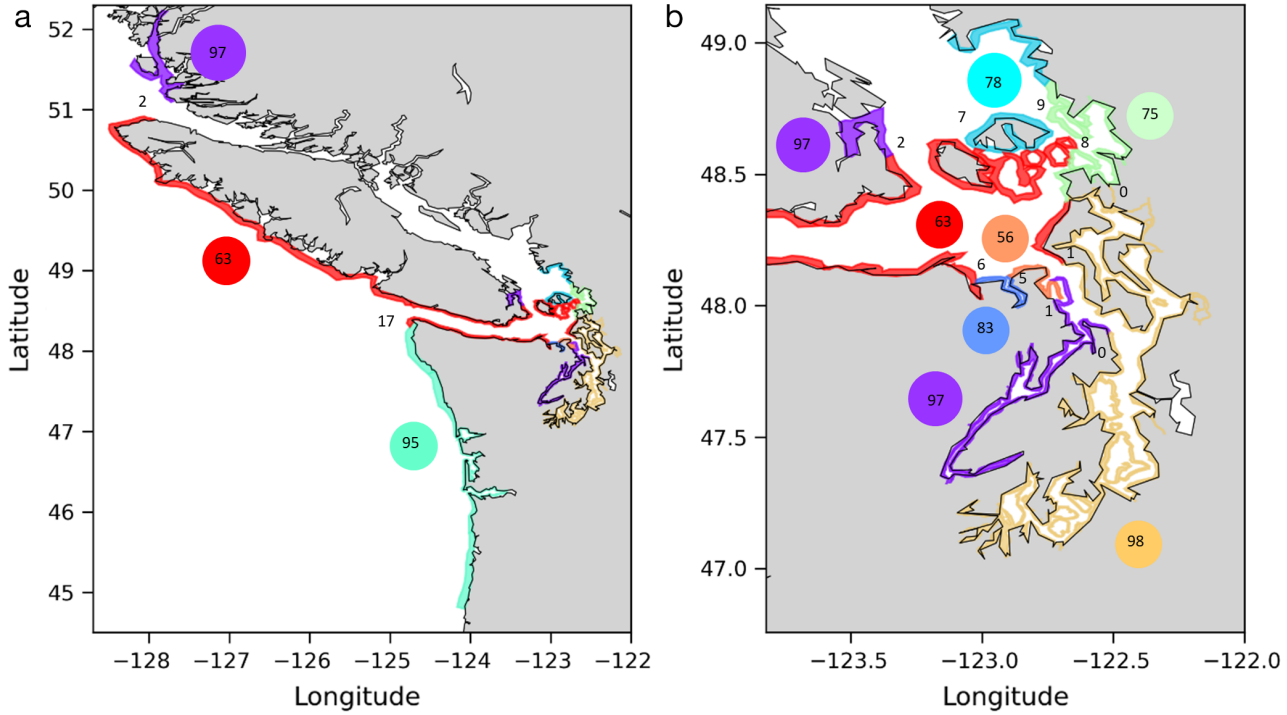

Fig. 8. Proposed management areas that optimize the algorithm of Jacobi et al. (2012) for 8 areas (a). (b) Zoomed in view of the same figure on the Puget Sound. Different colors depict different areas that contain original zones from Fig. 2. Numbers between areas represent the mean percentage of European green crab larvae exchanged between 2 adjacent areas and numbers in circles represent the percentage of local retention for each of the areas with the same corresponding color

refluxed deep enough, it would move into the Salish Sea from the Pacific Ocean during the normal (summer) Strait of Juan de Fuca conditions. In the model simulations without DVM, a few larvae were transported into the Salish Sea, specifically from release zones located on the Washington Coast to N and S Strait of Juan de Fuca, Sequim Bay, Port Townsend Bay, San Juan Island, and Victoria, by mixing down and entering the Strait of Juan de Fuca at depth following the typical circulation pattern of the Strait (Thomson et al. 2007) (see Fig. S3). This does not occur with DVM, because, in the model, DVM forces the larvae to be at certain depths. In reality, DVM could be overpowered by sufficiently strong water currents and larvae could enter the Salish Sea as occurred with our model. Previous studies have explored other mechanisms for EGC invasion in the Salish Sea: contaminated shellfish beds, seasonal Strait of Juan de Fuca flow reversal, and influence of El Niño Southern Oscillation (Curtis et al. 2015, Brasseale et al. 2019, Du et al. 2024). In addition to those relevant mechanisms, our simulations indicate the possibility that larvae may have entered the Salish Sea after mixing down to the eastward flow of the Strait of Juan de Fuca and then mixing up within the Salish Sea to settle successfully.

The high larval connectivity of EGC along the Pacific Coast can be explained by the California Current system. Due to the California Current system, water is moving north and south year-round at different distances from the coast via the Coastal Jet (south in summer along the coast), Davidson Current (north during winter along the water surface off the coast), California Undercurrent (north in subsurface off the coast) and the California Current (south off the coast) (Hickey 1979). Thus, larvae can be transported in either direction along the coast year-round (Behrens Yamada et al. 2021). Both larvae exiting the Salish Sea and larvae traveling north from the coast are being transported by the currents towards West Vancouver Island, explaining the high larval settlement in this area. The influence of the wind systems and the Columbia River plume coastal current is also likely to be a large contributor to this northward spread of larvae (Beutel & Allen 2024). The San Juan Islands region can be described as a hotspot of larval connectivity for EGC because this is a mostly closed sea, and thus larvae become trapped in the region (Premathilake & Khangaonkar 2022). These connected regions should be considered in the management of EGC, which will be explored further below. Model results also showed consistent larval connectivity of EGC throughout most of the Salish Sea and surrounding waters. High values of transport success were also noted from the model, highlighting zones of local retention for EGC larvae.

Several zones with high local larval retention of EGC were identified from the model, including Hakai Protected Area, Hood Canal, Discovery Bay, West Vancouver Island, and Saanich Inlet. The West Vancouver Island zone is large, fully exposed to the coast, and receives larvae from various zones, including itself. The Hakai Protected Area, Hood Canal, Discovery Bay, and Saanich Inlet zones receive most larvae locally and have constraining physical characteristics that may limit water flow. As the model is set to allow the larvae to settle if they are within a settlement zone after 30 d, a zone with high local retention indicates the residence time of that zone is longer than 30 d. Thus, our model predicts that the Hakai Protected Area, Hood Canal, Discovery Bay, and Saanich Inlet zones have residence times longer than 30 d. These results match previous studies on residence time in the Hood Canal (MacCready et al. 2021, Premathilake & Khangaonkar 2022). The geographic shape of the Hood Canal, Discovery Bay, and Saanich Inlet zones likely explains these observations, but the Hakai Protected Area may be particularly susceptible to local retention of EGC larvae because of its location directly on the Pacific coast and north of Vancouver Island. There was an eddy just south of the Hakai Protected Area zone during the simulation on 1 April 2020, which likely retained larvae within the zone. We observed this eddy in the other simulations as well. Larval connectivity patterns of EGC were observed to change with different hydrodynamic conditions and vary annually. Transport time scales of basins and sub-basins across Puget Sound may influence the spreading and patterns of EGC migration into inner Puget Sound as larvae retention times are significantly dependent on residence and flushing times. As a result of the complex circulation patterns described above, the basins and sub-basins of Puget Sound exhibit spatially and seasonally varying residence and flushing times (Premathilake & Khangaonkar 2022), a fact that indicates the dominant role played by the circulation of the Salish Sea with respect to EGC larvae transport.

Interannual variability was observed for the number of larvae that settled at each settlement zone, the number of larvae that successfully settled from each release zone, and the total transport success. El Niño and La Niña climate patterns are expected to influence EGC invasion due to their effects on ocean currents and water temperature (Behrens Yamada et al. 2021). In the Pacific Northwest, El Niño years are

warmer and with less precipitation, and La Niña years are colder with more precipitation. Thus, there should be less larval dispersal of EGC in La Niña years due to reduced crab activity with cold temperatures and increased larval flushing to the ocean due to higher river flow in the estuary (Behrens Yamada et al. 2021). There is some evidence for the influence of these climate patterns in our results: 2014 and 2015 were El Niño years and had higher larval transport success than 2016 and 2017, which were La Niña years. Transport success decreased from 2020 to 2022 which were La Niña years, but transport success was still very high in general in 2020 and 2021. Also, 2019 had the highest transport success but was not associated with a climate event. Further, Du et al. (2024) looked extensively at the influence of El Niño and predicted increased larval success within the Salish Sea with stronger El Niño events. Since temperature was not included in our model, the influence of these climate patterns on EGC larval dispersal is likely not fully considered in our study. Other parameters, such as larval behavior, were included, however, and slightly changed larval connectivity.

When DVM was included, the overall transport success of EGC larvae was slightly reduced, and less larval settlement was observed in the Salish Sea and surrounding waters. However, larval connectivity patterns were qualitatively similar. Without DVM, most larvae remain within the top 30 m of the water column, with occasional larvae reaching depths as deep as 160 m. Since our DVM definition maintains the larvae depth at either 3 or 15 m below the surface, in both cases, larvae are in the surface waters and there is no significant difference in transport success between including and neglecting DVM. Previous modeling studies of EGC larval dispersal included DVM and did not compare to results without DVM (Brasseale et al. 2019). Du et al. (2024) compared with and without DVM but included temperature dependence. Similar to our study, larvae tend to remain in the top 15 m of the water column without DVM. Our results indicate that if larvae remain in the surface waters, they exhibit overall similar transport success as larvae with DVM.

The dispersal of EGC larvae within the Salish Sea and surrounding waters between regions of the USA and Canada reveals the transnational connectivity of the species. In the Salish Sea region, EGC management is divided between the USA and Canada and between US states. The Washington Department of Fish and Wildlife (WDFW) is currently managing EGC in Washington State by geographic region and feature (WDFW 2024). Their definition does not compare with the connectivity patterns of EGC highlighted in our study. In our study, 8 highly connected areas of EGC are identified in the region. It is important to note that habitat can influence management recommendations (Garavelli et al. 2016), and since habitat is not considered in this study, the following recommendations are subject to change with habitat considerations. The partitioning into independent areas provides a new vision for regional management to coordinate management efforts of EGC between states and countries. In this new proposal, the highly connected area between the Canada and United States highlights the importance of working across country borders on the management of EGC. Further, as the Pacific Coast is highly connected, it should be treated as one management area (including the Oregon Coast). The locations of the highest local retention highlight the effects of the water circulation on larval transport. Coordinating management efforts of EGC within each identified independent highly connected area could minimize the larval dispersal of the species and therefore its invasion.

As with any modeling study, there are limitations to this work. A lower-resolution version of the SSM (average cell size ≈800 m in Puget Sound and ≈3000 m in the Strait of Juan De Fuca) was used in this study with the release of 10 000 virtual larvae per release event. Results from this study are useful to assess regional patterns of larval connectivity for EGC and to gain a better understanding of the influence of environmental conditions on larval dispersal. Because low-resolution hydrodynamic models do not accurately capture relevant coastal processes for larval retention, future work will consider the use of the high-resolution version of the SSM, particularly in regions where local retention was highlighted in this study. Furthermore, the ideal timestep in a particle-tracking model largely depends on the grid size. This study employs a timestep sufficient for capturing the overall larval connectivity of EGC in the system, but not for diagnosing all characteristics of larval dynamics in highly refined portions of the grid. Specifically, a sensitivity analysis with timesteps of 15, 30, and 60 min revealed that the overall connectivity patterns remain for all timesteps but a very small amount of additional connectivity does occur in the tighter regions of the domain, such as the North Puget Sound region which includes the San Juan Islands and Discovery Bay, with a reduced timestep. To remain computationally reasonable for a study of this spatial and temporal scale, a 30 min timestep was selected. Future work focusing on larval dynamics in a smaller

portion of the domain or utilizing a higher-resolution grid should adjust the timestep accordingly.

Another limitation of our study was the definition of the release and settlement areas. Larval trajectories show that larvae travel into the Strait of Georgia, but no settlement zones were included in this region in our model to keep the focus on Washington waters. The release and settlement zones defined in the model vary in size and cover wide regions. This variability was accounted for by normalizing the values in the connectivity matrices to the number of larvae released.

This study did not utilize any data on current EGC locations in its development or validation and focused on the larval connectivity of EGC in the entire region via model simulation only. Active adult trapping efforts are occurring in the region by federal and state agencies, private industry, and Tribal Nations, providing an abundance of data. The inclusion of those data in further modeling studies would allow for validation of the larval connectivity results. While using simulation results only allows us to study hypothetical scenarios and explore the larval connectivity of the region, specific management applications would benefit from including those data.

The management areas of EGC identified in our study provide an initial alternative plan based on the biology of the species and should be further evaluated using a high-resolution model with other biological parameters (e.g. larval growth, larval mortality). Finally, EGC habitat was not considered in the study. EGC megalopae select physically complex habitats (i.e. not bare substrate) for settlement (Hedvall et al. 1998). Juvenile crabs similarly inhabit complex habitats due to the refuge value from predation (Hedvall et al. 1998). Considering our model results, EGC are not expected to settle in certain portions of the Strait of Juan de Fuca due to habitat unsuitability. Thus, a regional management plan should also consider habitat suitability for larval settlement.

5. CONCLUSION

The larval connectivity results from this study can be used together with existing EGC monitoring data to provide helpful insights for invasive species management: connected areas within the Salish Sea and surrounding waters highlight potential future sources of invasion and should be managed accordingly. For example, if a zone within a connected area identifies an invasive species, the other zones within that area can adapt their trapping efforts. For the case of EGC in the Salish Sea region, this study identified 8 management areas based on a rigorous connectivity analysis of larval dispersal simulations during EGC spawning months from 2013 to 2022. Further, we investigated interannual patterns of the connectivity results and identified patterns that influenced the EGC invasion thus far. We also assessed the influence of larval behavior on connectivity within the region. Understanding past invasions and the influence of model parameters are critical to adapting future management scenarios.

Acknowledgements. We acknowledge the United States Environmental Protection Agency for funding this study (USEPA Federal Grant No. O2305-068-089-008183). Special thanks to Emily Grason and Sean McDonald for their discussions on model setup. Thanks also to Katie Morrice and the anonymous reviewers for reviewing a previous version of this paper and greatly improving its quality.

LITERATURE CITED

Amorim FN, Caetano M, Bastos L, Iglesias I (2024) Deep-sea mining rock-fragment dispersal scenarios associated with submesoscale forcings: a case study in the Atlantic. Heliyon 10:e34174

Banas NS, McDonald PS, Armstrong DA (2009) Green crab larval retention in Willapa Bay, Washington: an intensive Lagrangian modeling approach. Estuaries Coasts 32: 893–905

Barrier N, Verley P, Andres G, Lett C (2023) Ichthyop: A Lagrangian tool for modelling ichthyoplankton dynamics. (3.3.16). Zenodo. https://doi.org/10.5281/zenodo.7986365

Behrens Yamada S, Kosro P (2010) Linking ocean conditions to year class strength of the invasive European green crab, *Carcinus maenas*. Biol Invasions 12:1791–1804

Behrens Yamada S, Peterson WT, Kosro PM (2015) Biological and physical ocean indicators predict the success of an invasive crab, *Carcinus maenas*, in the northern California Current. Mar Ecol Prog Ser 537: 175–189

Behrens Yamada S, Thomson RE, Gillespie GE, Norgard TC (2017) Lifting barriers to range expansion: The European green crab *Carcinus maenas* (Linnaeus, 1758) enters the Salish Sea. J Shellfish Res 36:201–208

Behrens Yamada S, Fisher JL, Kosro PM (2021) Relationship between ocean ecosystem indicators and year class strength of the invasive European green crab (*Carcinus maenas*). Prog Oceanogr 196:102618

Berrill M (1982) The life cycle of the green crab *Carcinus maenas* at the northern end of its range. J Crustac Biol 2: 31–39

Beutel B, Allen SE (2024) Seasonal and interannual Salish Sea inflow origins using Lagrangian tracking. J Geophys Res Oceans 129:e2023JC020106

Brasseale E, Grason EW, McDonald PS, Adams J, MacCready P (2019) Larval transport modeling support for

identifying population sources of European green crab in the Salish Sea. Estuaries Coasts 42:1586–1599

Chen C, Liu H, Beardsley RC (2003) An unstructured grid, finite-volume, three-dimensional, primitive equations ocean model: application to coastal ocean and estuari es. J Atmos Ocean Technol 20:159–186

Criales MM, Chérubin L, Gandy R, Garavelli L, Ghannami MA, Crowley C (2019) Blue crab larval dispersal highlights population connectivity and implications for fishery management. Mar Ecol Prog Ser 625:53–70

Curtis LJF, Curtis DL, Matkin H, Thompson M and others (2015) Evaluating transfers of harvested shellfish products, from the west to the east coast of Vancouver Island, as a potential vector for European green crab (*Carcinus maenas*) and other non-indigenous invertebrate species. DFO Can Sci Advis Sec Res Doc 2015/014. https://waves-vagues.dfo-mpo.gc.ca/library-bibliotheque/359729.pdf

Darling JA, Bagley MJ, Roman J, Tepolt CK, Geller JB (2008) Genetic patterns across multiple introductions of the globally invasive crab genus *Carcinus*. Mol Ecol 17: 4992–5007

Dawirs RR (1985) Temperature and larval development of *Carcinus maenas* (Decapoda) in the laboratory; predictions of larval dynamics in the sea. Mar Ecol Prog Ser 24:297–302

deRivera C, Hitchcock N, Teck S, Steves B, Hines A, Ruiz G (2007) Larval development rate predicts range expansion of an introduced crab. Mar Biol 150:1275–1288

DiBacco C, Therriault TW (2015) Reproductive periodicity and larval vertical migration behavior of European green crab *Carcinus maenas* in a non-native habitat. Mar Ecol Prog Ser 536:123–134

Du J, Tepolt CK, Grason EW, McDonald PS, Jia Y, Zhang WG (2024) Dispersal pathways of European green crab larvae into and throughout the eastern Salish Sea. Prog Oceanogr 223:103245

Garavelli L, Kaplan DM, Colas F, Stotz W, Yannicelli B, Lett C (2014) Identifying appropriate spatial scales for marine conservation and management using a larval dispersal model: the case of *Concholepas concholepas* (loco) in Chile. Prog Oceanogr 124:42–53

Garavelli L, Colas F, Verley P, Kaplan DM, Yannicelli B, Lett C (2016) Influence of biological factors on connectivity patterns for *Concholepas concholepas* (loco) in Chile. PLOS ONE 11:e0146418

Giddings SN, MacCready P (2017) Reverse estuarine circulation due to local and remote wind forcing, enhanced by the presence of along-coast estuaries. J Geophys Res Oceans 122:10184–10205

Gillespie GE, Norgard TC, Anderson ED, Haggarty DR, Phillips AC (2015) Distribution and biological characteristics of European green crab, *Carcinus maenas*, in British Columbia, 2006 - 2013. Can Tech Rep Fish Aquat Sci 3120. https://waves-vagues.dfo-mpo.gc.ca/library-bibliotheque/357455.pdf

Grason EW, Adams JW, Litle K, McDonald PS, Dalton P (2017) European green crab early detection and monitoring. Final Report WSG-TR 16-07. Washington Sea Grant, Seattle, WA

Grason EW, McDonald PS, Adams J, Litle K, Apple JL, Pleus A (2018) Citizen science program detects range expansion of the globally invasive European green crab in Washington State. Manag Biol Invasions 9:39–47

Grosholz ED, Drill SL, McCann L, Bimrose K (2021) Engaging the importance of community scientists in the management of an invasive marine pest. Calif Agric 75:40–45

Hedvall O, Moksnes PO, Pihl L (1998) Active habitat selection by megalopae and juvenile shore crabs *Carcinus maenas*: a laboratory study in an annular flume. Hydrobiologia 375:89–100

Hickey BM (1979) The California current system—hypotheses and facts. Prog Oceanogr 8:191–279

Jacobi MN, André C, Döös K, Jonsson PR (2012) Identification of subpopulations from connectivity matrices. Ecography 35:1004–1016

Khangaonkar T, Yun SK (2023) Estuarine nutrient pollution impact reduction assessment through euphotic zone avoidance/bypass considerations. Front Mar Sci 10: 1192111

Khangaonkar T, Long W, Xu W (2017) Assessment of circulation and inter-basin transport in the Salish Sea including Johnstone Strait and Discovery Islands pathways. Ocean Model 109:11–32

Khangaonkar T, Nugraha A, Xu W, Long W and others (2018) Analysis of hypoxia and sensitivity to nutrient pollution in Salish Sea. J Geophys Res Oceans 123: 4735–4761

Kouba A, Oficialdegui FJ, Cuthbert RN, Kourantidou M and others (2022) Identifying economic costs and knowledge gaps of invasive aquatic crustaceans. Sci Total Environ 813:152325

Leignel V, Stillman JH, Baringou S, Thabet R, Metais I (2014) Overview on the European green crab *Carcinus* spp. (Portunidae, Decapoda), one of the most famous marine invaders and ecotoxicological models. Environ Sci Pollut Res Int 21:9129–9144

Lett C, Verley P, Mullon C, Parada C, Brochier T, Penven P, Blanke B (2008) A Lagrangian tool for modelling ichthyoplankton dynamics. Environ Model Softw 23:1210–1214

Lett C, Nguyen-Huu T, Cuif M, Saenz-Agudelo P, Kaplan DM (2015) Linking local retention, self-recruitment, and persistence in marine metapopulations. Ecology 96: 2236–2244

MacCready P, Geyer WR (2024) Estuarine exchange flow in the Salish Sea. J Geophys Res Oceans 129:e2023JC 020369

MacCready P, McCabe RM, Siedlecki SA, Lorenz M and others (2021) Estuarine circulation, mixing, and residence times in the Salish Sea. J Geophys Res Oceans 126:e2020JC016738

Marchessaux G, Chevalier C, Mangano MC, Sarà G (2023) Larval connectivity of the invasive blue crabs *Callinectes sapidus* and *Portunus segnis* in the Mediterranean Sea: a step toward improved cross border management. Mar Pollut Bull 194:115272

Matheson K, McKenzie CH, Gregory RS, Robichaud DA, Bradbury IR, Snelgrove PVR, Rose GA (2016) Linking eelgrass decline and impacts on associated fish communities to European green crab *Carcinus maenas* invasion. Mar Ecol Prog Ser 548:31–45

Muller C, Lett C, Porri F, Pattrick P and others (2024) Coastal connectivity of an abundant inshore fish species: model–data comparison along the southern coast of South Africa. Mar Ecol Prog Ser 731:89–104

Olson JK, Lambourn DM, Huggins JL, Raverty S, Scott AA, Gaydos JK (2021) Trends in propeller strike-induced mortality in harbor seals (*Phoca vitulina*) of the Salish Sea. J Wildl Dis 57:689–693

Pineda J, Hare J, Sponaugle S (2007) Larval transport and dispersal in the coastal ocean and consequences for population connectivity. Oceanography 20:22–39

Premathilake L, Khangaonkar T (2022) Explicit quantification of residence and flushing times in the Salish Sea using a sub-basin scale shoreline resolving model. Estuar Coast Shelf Sci 276:108022

Queiroga H (1996) Distribution and drift of the crab *Carcinus maenas* (L.) (Decapoda, Portunidae) larvae over the continental shelf off northern Portugal in April 1991. J Plankton Res 18:1981–2000

Queiroga H, Moksnes PO, Meireles S (2002) Vertical migration behaviour in the larvae of the shore crab *Carcinus maenas* from a microtidal system (Gullmarsfjord, Sweden). Mar Ecol Prog Ser 237:195–207

Roy HE, Pauchard A, Stoett P, Renard Truong T and others (2023) IPBES invasive alien species assessment: summary for policymakers (Version 3). Zenodo https://doi.org/10.5281/zenodo.10127924

Soontiens N, Allen SE, Latornell D, Le Souëf K and others (2016) Storm surges in the Strait of Georgia simulated with a regional model. Atmos-Ocean 54:1–21

Sutherland DA, MacCready P, Banas NS, Smedstad LF (2011) A model study of the Salish Sea estuarine circulation. J Phys Oceanogr 41:1125–1143

Thomson RE, Mihály SF, Kulikov EA (2007) Estuarine versus transient flow regimes in Juan de Fuca Strait. J Geophys Res 112:C09022

WDFW (Washington Department of Fish and Wildlife) (2024) European Green Crab Hub. https://wdfw-egc-hub-wdfw.hub.arcgis.com/

Young AM, Elliott JA (2020) Life history and population dynamics of green crabs (*Carcinus maenas*). Fishes 5:4

Zeng C, Naylor E (1996) Synchronization of endogenous tidal vertical migration rhythms in laboratory-hatched larvae of the crab *Carcinus maenas*. J Exp Mar Biol Ecol 198:269–289

Editorial responsibility: Alejandro Gallego, Aberdeen, UK
Reviewed by: T. Adams and 2 anonymous referees
Submitted: June 18, 2024; Accepted: December 10, 2024
Proofs received from author(s): February 7, 2025